Source Parameters of the Shallow 2012 Brawley Earthquake, Imperial Valley

Risheng Chu and Don V. Helmberger
Seismological Laboratory, California Institute of Technology, Pasadena, CA 91125

We thank the Gordon and Betty Moore Foundation for financial support.

Abstract: Resolving earthquake parameters, especially depth, is difficult for events occurring within basins because of issues involved with separating source properties from propagational path effects. Here, we demonstrate some advantages of using a combination of teleseismic and regional waveform data to improve resolution following a bootstrapping approach. SS-S differential arrivals from a foreshock are used to determine a local layered model which can then be used to model the depth phases; pP, sP, and sS. Using the Cut-and-Paste (CAP) method where all strike (θ), dip (δ), rake (λ) and depth variations are sampled for several crustal models. Regional data proves the most reliable at fixing the strike while the depth is better constrained by teleseismic data. Weighted solutions indicate a nearly pure strike-slip mechanism (θ = 59 ± 1°) with a centroid depth of ~4.0 km and an Mw of 5.4 for the mainshock of the 2012 Brawley earthquake.

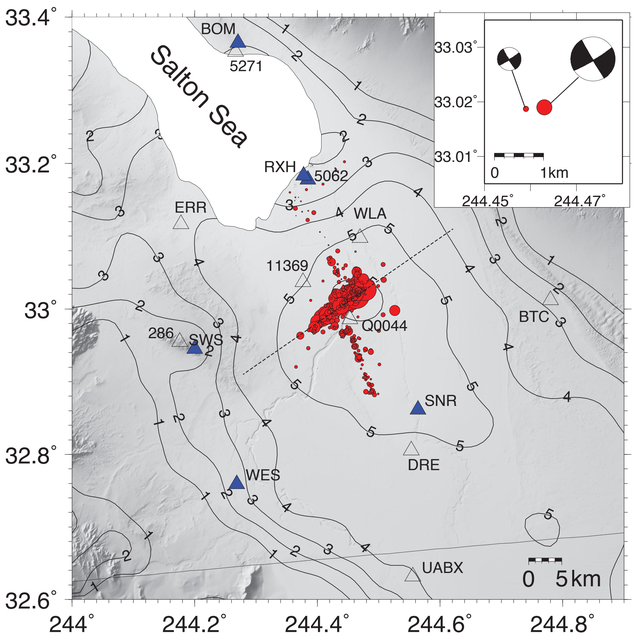

Fig. 1: Hypocenters of the 26 August 2012 Brawley earthquake swarm. Red dots denote relocated earthquakes from Hauksson et al. [2012]. The contours show the depth of basement rocks from SCEC CVM 4.0 model with depth labeled at an interval of 1 km [Magistrale et al., 2000]. Solid blue triangles are local seismic stations whose waveforms are modeled in this study. The dashed line denotes the inverted strike direction. The inset shows the locations and focal mechanisms of the Mw 3.9 foreshock and the mainshock.

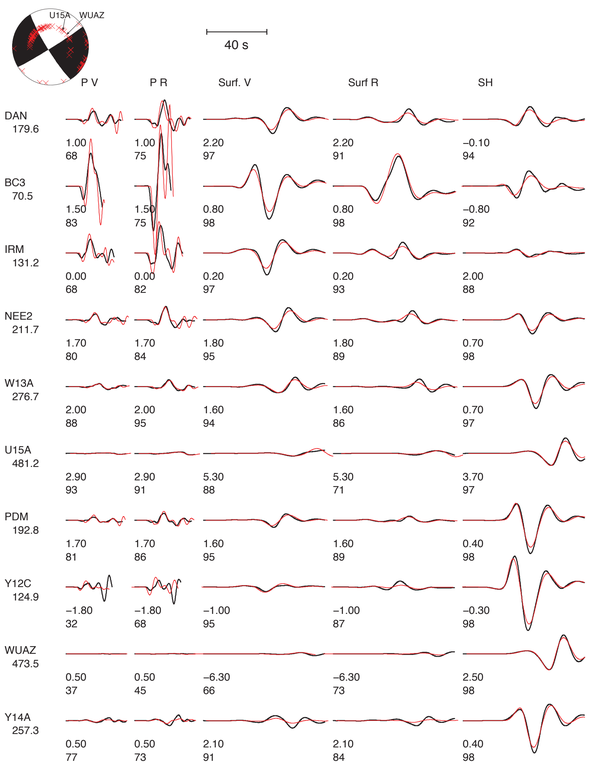

Fig. 2. Regional Cut-and-Paste inversion of the Brawley earthquake. The waveforms are arranged according to their azimuths. The Pnl and surface waves are filtered using corner frequencies of 0.02-0.2 Hz and 0.01-0.05 Hz, respectively. The station names are given on the right along with the distance in km. The best-fit mechanism is a strike-slip faulting at the depth of 5.5 km. The velocity model used here is SC (shown in Fig. 4). Observed and synthetic displacement waveforms are shown as black and red trace, respectively. The two numbers beneath each trace are its time shift relative to the synthetic segments generated from the 1D model to match the data and the cross-correlation coefficient. Note the stations with low amplitude in the P nodal direction (WUAZ), and S nodal direction (IRM).

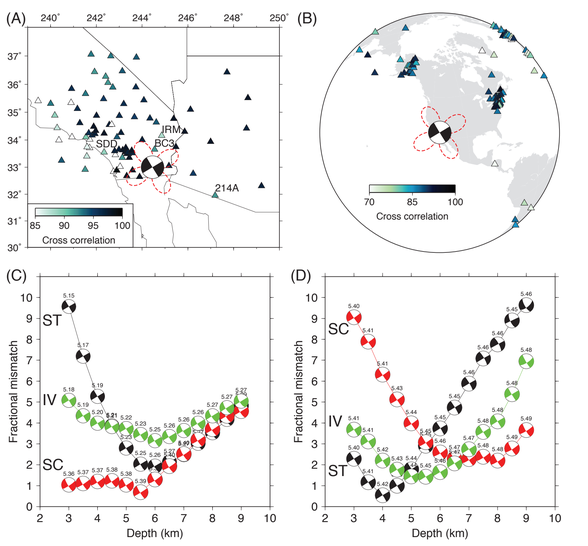

Fig. 3. Regional and teleseismic CAP inversions. (A) and (B) display cross-correlation coefficient (CC) for regional inversion using SC model and teleseismic inversion using ST model, respectively. We have included the SH radiation pattern as the red dashed curves. (C) and (D) show the misfits as a function of centroid depth for the southern California model SC, the Imperial Valley model IV, and the Salton Trough model ST for the regional and teleseismic inversions, respectively. Note strong minimums found for the ST model, especially at teleseismic distances. Teleseismic t* for P and SH waves are 0.8 and 3.2 s, respectively [Chu et al., 2012].

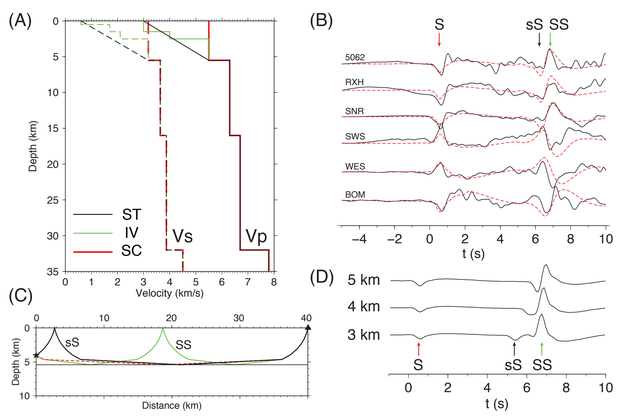

Fig. 4. 1D Salton Trough shear-velocity model. (A) A comparison of 1D velocity models between southern California model SC (red), Imperial Valley model IV (green), and Salton Trough model ST (black). Because of the deep basin structure, multiple surface reflections sS and SS are observed following the direct S. These three arrivals are indicated by arrows in (B) and their ray paths are given in (C). Synthetic waveforms for events with depth at 3 km, 4 km, and 5 km suggest that sS is easily affected by earthquake depth and SS is determined mainly by the basin velocity structure (D). Synthetics from velocity model ST (dashed lines), bandpass filtered between 0.1 and 2.0 Hz, is plotted against tangential displacement data in (B). Both data and synthetics are aligned at the arrivals of the direct S.

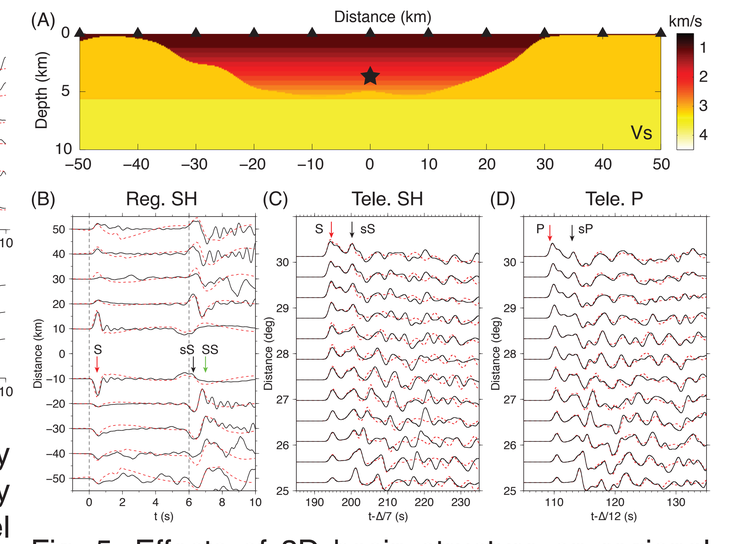

Fig. 5. Effects of 2D basin structure on regional and teleseismic waveforms. (A) The basin structure is constructed using the depth of basement rocks along the strike from Magistrale et al. [2000] (Fig. 4). Inside the basin, the velocities are those from model ST. The background velocities are the models SC for the crust and AK135 for the mantle [Kennett et al., 1995]. The star represents the hypocenter of the Brawley earthquake. (B) Comparison of regional SH waves from 2D basin structure (black lines) and those from 1D model SC (dashed lines). All synthetics are bandpass filtered using corner frequencies of 0.1 and 2.0 Hz. The direct S and its surface reflections sS and SS are labeled. (C) and (D) show comparisons of teleseismic SH and P waves from 2D (black lines) and 1D (dashed lines) basin structures.

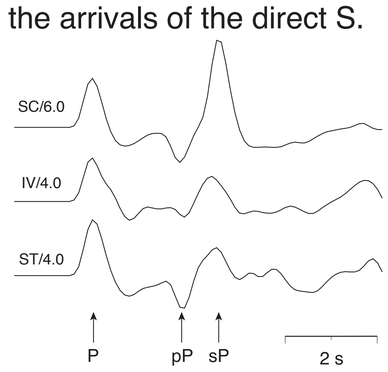

Fig.6. Synthetic P-wave Green's functions for a strike-slip earthquake using velocity models SC (top), IV (middle), and ST (bottom). The station has a distance of 30°. The arrows indicate the direct P and the depth phases pP and sP. The calculations have different depths (numbers after the model names) to ensure the similar sP-P arrival times.

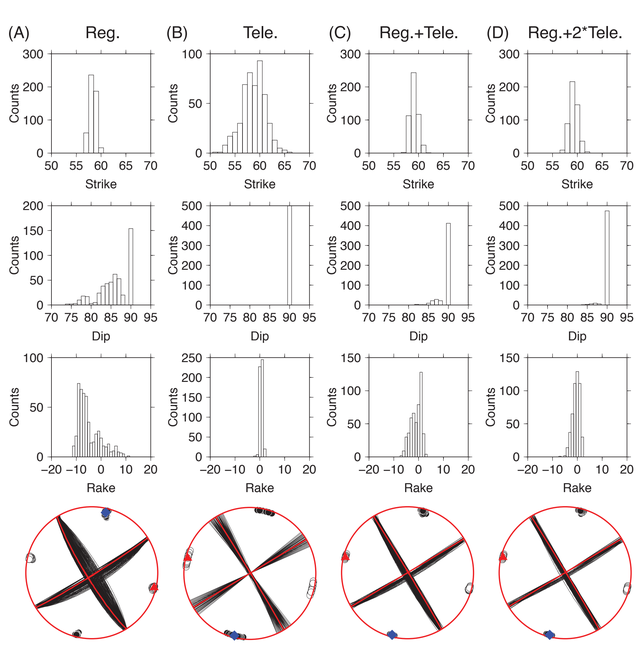

Fig. 7: Bootstrapping of CAP inversions. Distribution of strike, dip, and rake from 500 solutions are displayed for (A) regional and (B) teleseismic inversions, respectively. Two joint inversions using both regional and teleseismic data are displayed in (C) and (D) with different weight of teleseismic data. Nodal planes (black lines) and P/T axis (solid and open circles) of the 500 mechanisms are also shown together with nodal planes (thick lines) and P/T axis (diamonds and triangles) of the mechanism from the original dataset.

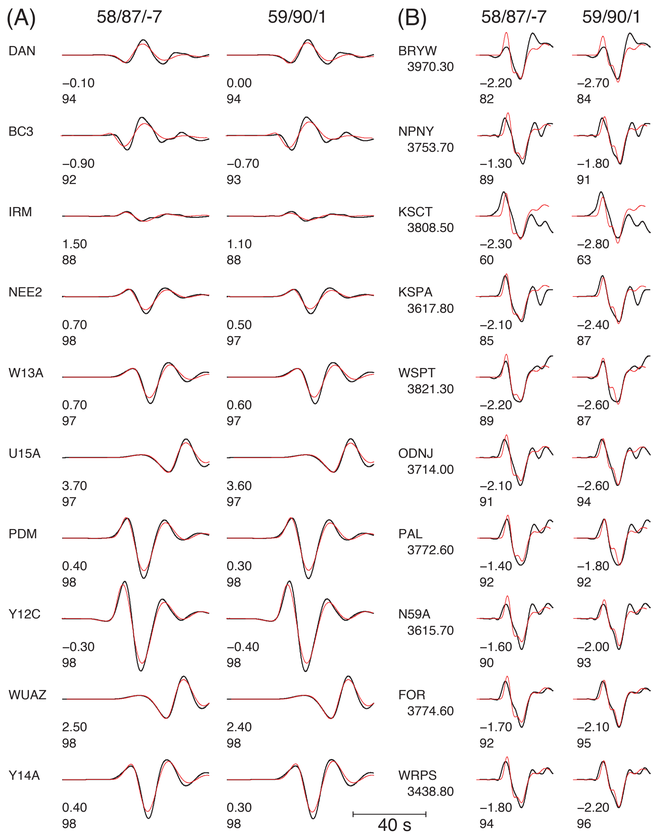

Fig. 8. Sensitivity of regional and teleseismic data on focal mechanisms. Comparison of synthetic (red) and observed data (black) for (A) regional Love waves and (B) teleseismic SH waves. For each dataset, synthetic waveforms are calculated using focal mechanisms from regional CAP solution (58/87/-7, left) and teleseismic CAP solution (59/90/1, right).